March 2013

Sediment Profile Imaging Report

Demonstration of *in-situ* Treatment of Contaminated Sediments with Reactive Amendments: Baseline Survey




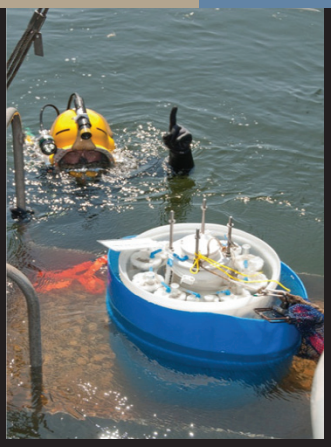


Prepared for

Environ International Corporation
333 West Wacker Drive
Suite 2700
Chicago, IL 60606-1220

Client Contract Number 2129692A

Prepared by

Germano & Associates, Inc.
12100 SE 46th Place
Bellevue, WA 98006

Sediment Profile Imaging Report

DEMONSTRATION OF *IN-SITU* TREATMENT OF CONTAMINATED SEDIMENTS WITH REACTIVE AMENDMENTS: BASELINE SURVEY

Prepared for

Environ International Corporation
333 West Wacker Drive
Suite 2700
Chicago, IL 60606-1220

Client Contract Number 2129692A

Prepared by

Germano & Associates, Inc.
12100 SE 46th Place
Bellevue, WA 98006

March, 2013

TABLE OF CONTENTS

LIST OF FIGURES

1.0
INTRODUCTION

As part of a multidisciplinary effort to investigate the feasibility of treating contaminated sediments in active Department of Defense (DoD) harbors, Germano & Associates, Inc. (G&A) performed a Sediment Profile Imaging (SPI) survey around Pier 7 at the Puget Sound Naval Shipyard & Intermediate Maintenance Facility (PSNS & IMF), Bremerton site. The purpose of the SPI survey was to document baseline conditions at a total of 42 stations before the reactive amendment was placed on the sediment surface.

2.0
MATERIALS AND METHODS

Between August 16-17, 2012, scientists from G&A collected a series of sediment profile images at a total of 42 stations (Figure 1). Two different versions of an Ocean Imaging Systems Model 3731 sediment profile camera were used for this survey; a standard SPI system using a surrounding frame that was deployed from a vessel (Figure 2), and a hand-held aluminum SPI system (Figure 3) deployed by PSNS & IMF divers for stations that were located under the pier and inaccessible for sampling with a boat. Stations were arranged in an orthogonal grid of seven rows with six stations in each row, with spacing between stations of approximately 8 meters; half the stations (positions #1, 2, and 3 in each row) were sampled by divers using the hand-held SPI unit, while any remaining stations that were not under the pier (including all of row #7) were sampled from the vessel using the frame-deployed SPI system.

SPI was developed almost four decades ago as a rapid reconnaissance tool for characterizing physical, chemical, and biological seafloor processes and has been used in numerous seafloor surveys throughout North America, Asia, Europe, and Africa (Rhoads and Germano 1982, 1986, 1990; Revelas et al. 1987; Diaz and Schaffner, 1988; Valente et al. 1992; Germano et al. 2011). The sediment profile camera works like an inverted periscope. A Nikon D7000 16.2-megapixel SLR camera with two 8-gigabyte secure digital (SD) cards is mounted horizontally inside a watertight housing on top of a wedge-shaped prism. The prism has a Plexiglas® faceplate at the front with a mirror placed at a 45° angle at the back. The camera lens looks down at the mirror, which is reflecting the image from the faceplate. The prism has an internal strobe mounted inside at the back of the wedge to provide illumination for the image; this chamber is filled with distilled water, so the camera always has an optically clear path. This wedge assembly is mounted on a moveable carriage within a stainless steel frame. The frame is lowered to the seafloor on a winch wire, and the tension on the wire keeps the prism in its “up” position. When the frame comes to rest on the seafloor, the winch wire goes slack (see Figure 2) and the camera prism descends into the sediment at a slow, controlled rate by the dampening action of a hydraulic piston so as not to disturb the sediment-water interface. On the way down, it trips a trigger that activates a time-delay circuit of variable length (operator-selected) to allow the camera to penetrate the seafloor before any image is taken. The knife-sharp edge of the prism transects the sediment, and the prism penetrates the bottom. The strobe is discharged after an appropriate time delay to obtain a cross-sectional image of the upper 20 cm of the sediment column. The resulting images give the viewer the same perspective as looking through the side of an aquarium half-filled with sediment. After the first image is obtained at the first location, the camera is then raised up about 2 to 3 meters off the bottom to allow the strobe to recharge; a wiper blade mounted on the frame removes any mud adhering to the faceplate. The strobe recharges within 5 seconds, and the camera is ready to be lowered again for a replicate image.

Surveys can be accomplished rapidly by "pogo-sticking" the camera across an area of seafloor while recording positional fixes on the surface vessel.

The hand-held SPI system (Figure 3) works on the same design, except that there is no time delay once the watertight switch is activated by the diver after the prism is inserted into the sediment. There is no wiper blade on the hand-held system, so the diver needs to clean the faceplate of the camera prism manually with a scrub brush after each image is taken.

Two types of adjustments to the SPI system are typically made in the field: physical adjustments to the chassis stop collars on the frame-deployed system or adding/subtracting lead weights to the chassis to control penetration in harder or softer sediments, and electronic software adjustments to the Nikon D7000 to control camera settings. Camera settings (f-stop, shutter speed, ISO equivalents, digital file format, color balance, etc.) are selectable through a water-tight USB port on the camera housing and Nikon Control Pro® software. At the beginning of the survey, the time on both of the sediment profile cameras' internal data loggers was synchronized with the clock on the sampling vessel to local time. Details of the camera settings for each digital image are available in the associated parameters file embedded in the electronic image file; for this survey, the ISO-equivalent was set at 640. The additional camera settings used were as follows: shutter speed was 1/250, f8, white balance set to flash, color mode to Adobe RGB, sharpening to none, noise reduction off, and storage in compressed raw Nikon Electronic Format (NEF) files (approximately 20 MB each). Electronic files were converted to high-resolution jpeg (14-bit) format files (49278 x 3264 pixels) using Nikon Capture NX2® software (Version 2.3.5.).

Three replicate images were taken at each station at the vessel-deployed frame stations, while 2 replicate images were taken by the divers at each of the under-pier stations; each SPI replicate is identified by the time recorded on the digital image file in the camera and in the field log on the vessel. The SD card was immediately surrendered at the completion of the survey to Navy security for review before the images could be released for public distribution. The unique time stamp on the digital image was then cross-checked with the time stamp recorded in the written sample logs. After the images were cleared by PSNS & IMF for release, they were re-named with the appropriate station name based on the time stamp on each image.

Test exposures of the Kodak® Color Separation Guide (Publication No. Q-13) were made on deck at the beginning of the survey to verify that all internal electronic systems were working to design specifications and to provide a color standard against which final images could be checked for proper color balance. A spare camera and charged battery were carried in the field at all times to insure uninterrupted sample acquisition. After deployment of the camera at each station, the frame counter was checked to make sure that the requisite number of replicates had been taken. In addition, a prism penetration depth indicator on the camera frame was checked to verify that the optical prism had

actually penetrated the bottom to a sufficient depth. If images were missed (frame counter indicator or verification from digital download) or the penetration depth was insufficient (penetration indicator), chassis stops were adjusted and/or weights were added or removed, and additional replicate images were taken. Changes in prism weight amounts, the presence or absence of mud doors, and chassis stop positions were recorded for each replicate image.

Following completion of the field operations, the raw NEF image files were converted to high-resolution Joint Photographic Experts Group (jpeg) format files using the minimal amount of image file compression. Once converted to jpeg format, the intensity histogram (RGB channel) for each image was adjusted in Adobe Photoshop® to maximize contrast without distortion. The jpeg images were then imported to Sigmascan Pro® (Aspire Software International) for image calibration and analysis. Calibration information was determined by measuring 1-cm gradations from the Kodak® Color Separation Guide. This calibration information was applied to all SPI images analyzed. Linear and area measurements were recorded as number of pixels and converted to scientific units using the calibration information.

Measured parameters were recorded on a Microsoft® Excel© spreadsheet. G&A's senior scientist (Dr. J. Germano) subsequently checked all these data as an independent quality assurance/quality control review of the measurements before final interpretation was performed.

2.1 MEASURING, INTERPRETING, AND MAPPING SPI PARAMETERS

2.1.1 Prism Penetration Depth

The SPI prism penetration depth was measured from the bottom of the image to the sediment-water interface. The area of the entire cross-sectional sedimentary portion of the image was digitized, and this number was divided by the calibrated linear width of the image to determine the average penetration depth.

Prism penetration is a noteworthy parameter; if the number of weights used in the camera is held constant throughout a survey, the camera functions as a static-load penetrometer. Comparative penetration values from sites of similar grain size give an indication of the relative water content of the sediment. Highly bioturbated sediments and rapidly accumulating sediments tend to have the highest water contents and greatest prism penetration depths.

The depth of penetration also reflects the bearing capacity and shear strength of the sediments. Overconsolidated or relic sediments and shell-bearing sands resist camera penetration. Highly bioturbated, sulfitic, or methanogenic muds are the least

consolidated, and deep penetration is typical. Seasonal changes in camera prism penetration have been observed at the same station in other studies and are related to the control of sediment geotechnical properties by bioturbation (Rhoads and Boyer 1982). The effect of water temperature on bioturbation rates appears to be important in controlling both biogenic surface relief and prism penetration depth (Rhoads and Germano 1982).

2.1.2 Thickness of Depositional Layers

Because of the camera's unique design, SPI can be used to detect the thickness of depositional and dredged material layers. SPI is effective in measuring layers ranging in thickness from 1 mm to 20 cm (the height of the SPI optical window). During image analysis, the thickness of the newly deposited sedimentary layers can be determined by measuring the distance between the pre- and post-disposal sediment-water interface. Recently deposited material is usually evident because of its unique optical reflectance and/or color relative to the underlying material representing the pre-disposal surface. Also, in most cases, the point of contact between the two layers is clearly visible as a textural change in sediment composition, facilitating measurement of the thickness of the newly deposited layer.

Because this was the baseline survey, there were no measurements recorded for the thickness of the reactive amendment; this parameter will be measured in future surveys at this site.

2.1.3 Apparent Redox Potential Discontinuity Depth

Aerobic near-surface marine sediments typically have higher reflectance relative to underlying hypoxic or anoxic sediments. Surface sands washed free of mud also have higher optical reflectance than underlying muddy sands. These differences in optical reflectance are readily apparent in SPI images; the oxidized surface sediment contains particles coated with ferric hydroxide (an olive or tan color when associated with particles), while reduced and muddy sediments below this oxygenated layer are darker, generally gray to black (Fenchel 1969; Lyle 1983). The boundary between the colored ferric hydroxide surface sediment and underlying gray to black sediment is called the apparent redox potential discontinuity (aRPD).

The depth of the aRPD in the sediment column is an important time-integrator of dissolved oxygen conditions within sediment porewaters. In the absence of bioturbating organisms, this high reflectance layer (in muds) will typically reach a thickness of 2 mm below the sediment-water interface (Rhoads 1974). This depth is related to the supply rate of molecular oxygen by diffusion into the bottom and the consumption of that oxygen by the sediment and associated microflora. In sediments that have very high sediment oxygen demand (SOD), the sediment may lack a high reflectance layer even when the overlying water column is aerobic.

In the presence of bioturbating macrofauna, the thickness of the high reflectance layer may be several centimeters. The relationship between the thickness of this high reflectance layer and the presence or absence of free molecular oxygen in the associated porewaters must be considered with caution. The actual RPD is the boundary or horizon that separates the positive reduction potential (Eh) region of the sediment column from the underlying negative Eh region. The exact location of this Eh = 0 boundary can be determined accurately only with microelectrodes; hence, the relationship between the change in optical reflectance, as imaged with the SPI camera, and the actual RPD can be determined only by making the appropriate *in situ* Eh measurements. For this reason, the optical reflectance boundary, as imaged, was described in this study as the "apparent" RPD and it was mapped as a mean value. In general, the depth of the actual Eh = 0 horizon will be either equal to or slightly shallower than the depth of the optical reflectance boundary (Rosenberg et al., 2001). This is because bioturbating organisms can mix ferric hydroxide-coated particles downward into the bottom below the Eh = 0 horizon. As a result, the mean aRPD depth can be used as an estimate of the depth of porewater exchange, usually through porewater irrigation (bioturbation). Biogenic particle mixing depths can be estimated by measuring the maximum and minimum depths of imaged feeding voids in the sediment column. This parameter represents the particle mixing depths of head-down feeders, mainly polychaetes.

The rate of depression of the aRPD within the sediment is relatively slow in organic-rich muds, on the order of 200 to 300 micrometers per day; therefore this parameter has a long time constant (Germano and Rhoads 1984). The rebound in the aRPD is also slow (Germano 1983). Measurable changes in the aRPD depth using the SPI optical technique can be detected over periods of 1 or 2 months. This parameter is used effectively to document changes (or gradients) that develop over a seasonal or yearly cycle related to water temperature effects on bioturbation rates, seasonal hypoxia, SOD, and infaunal recruitment. Time-series RPD measurements following a disturbance can be a critical diagnostic element in monitoring the degree of recolonization in an area by the ambient benthos (Rhoads and Germano 1986).

The mean aRPD depth also can be affected by local erosion. The peaks of disposal mounds commonly are scoured by divergent flow over the mound. This scouring can wash away fines and shell or gravel lag deposits, and can result in very thin surface oxidized layer. During storm periods, erosion may completely remove any evidence of the aRPD (Fredette et al. 1988).

Another important characteristic of the aRPD is the contrast in reflectance at this boundary. This contrast is related to the interactions among the degree of organic loading, the bioturbation activity in the sediment, and the concentrations of bottom-water dissolved oxygen in an area. High inputs of labile organic material increase SOD and, subsequently, sulfate reduction rates and the associated abundance of sulfide end products. This results in more highly reduced, lower-reflectance sediments at depth and

higher aRPD contrasts. In a region of generally low aRPD contrasts, images with high aRPD contrasts indicate localized sites of relatively large inputs of organic-rich material such as phytoplankton, other naturally-occurring organic detritus, dredged material, or sewage sludge.

Because the determination of the aRPD requires discrimination of optical contrast between oxidized and reduced particles, it is difficult, if not impossible, to determine the depth of the aRPD in well-sorted sands of any size that have little to no silt or organic matter in them (Painter et al, 2007). When using SPI technology on sand bottoms, little information other than grain-size, prism penetration depth, and boundary roughness values can be measured; while oxygen has no doubt penetrated the sand beneath the sediment-water interface just due to physical forcing factors acting on surface roughness elements (Ziebis et al., 1996; Huettel et al., 1998), estimates of the mean aRPD depths in these types of sediments are indeterminate with conventional white light photography.

2.1.4 Infaunal Successional Stage

The mapping of infaunal successional stages is readily accomplished with SPI technology. These stages are recognized in SPI images by the presence of dense assemblages of near-surface polychaetes and/or the presence of subsurface feeding voids; both may be present in the same image. Mapping of successional stages is based on the theory that organism-sediment interactions in fine-grained sediments follow a predictable sequence after a major seafloor perturbation. This theory states that primary succession results in "the predictable appearance of macrobenthic invertebrates belonging to specific functional types following a benthic disturbance. These invertebrates interact with sediment in specific ways. Because functional types are the biological units of interest..., our definition does not demand a sequential appearance of particular invertebrate species or genera" (Rhoads and Boyer 1982). This theory is presented in Pearson and Rosenberg (1978) and further developed in Rhoads and Germano (1982) and Rhoads and Boyer (1982).

This continuum of change in animal communities after a disturbance (primary succession) has been divided subjectively into four stages: Stage 0, indicative of a sediment column that is largely devoid of macrofauna, occurs immediately following a physical disturbance or in close proximity to an organic enrichment source; Stage 1 is the initial community of tiny, densely populated polychaete assemblages; Stage 2 is the start of the transition to head-down deposit feeders; and Stage 3 is the mature, equilibrium community of deep-dwelling, head-down deposit feeders (Figure 4).

After an area of bottom is disturbed by natural or anthropogenic events, the first invertebrate assemblage (Stage 1) appears within days after the disturbance. Stage 1 consists of assemblages of tiny tube-dwelling marine polychaetes that reach population densities of 10^4 to 10^6 individuals per m^2. These animals feed at or near the sediment-water interface and physically stabilize or bind the sediment surface by producing a

mucous "glue" that they use to build their tubes. Sometimes deposited dredged material layers contain Stage 1 tubes still attached to mud clasts from their location of origin; these transported individuals are considered as part of the *in situ* fauna in our assignment of successional stages.

If there are no repeated disturbances to the newly colonized area, then these initial tube-dwelling suspension or surface-deposit feeding taxa are followed by burrowing, head-down deposit-feeders that rework the sediment deeper and deeper over time and mix oxygen from the overlying water into the sediment. The animals in these later-appearing communities (Stage 2 or 3) are larger, have lower overall population densities (10 to 100 individuals per m^2), and can rework the sediments to depths of 3 to 20 cm or more. These animals "loosen" the sedimentary fabric, increase the water content in the sediment, thereby lowering the sediment shear strength, and actively recycle nutrients because of the high exchange rate with the overlying waters resulting from their burrowing and feeding activities.

In dynamic estuarine and coastal environments, it is simplistic to assume that benthic communities always progress completely and sequentially through all four stages in accordance with the idealized conceptual model depicted in Figure 3. Various combinations of these basic successional stages are possible. For example, secondary succession can occur (Horn, 1974) in response to additional labile carbon input to surface sediments, with surface-dwelling Stage 1 or 2 organisms co-existing at the same time and place with Stage 3, resulting in the assignment of a "Stage 1 on 3" or "Stage 2 on 3" designation.

While the successional dynamics of invertebrate communities in fine-grained sediments have been well-documented, the successional dynamics of invertebrate communities in sand and coarser sediments are not well-known. Subsequently, the insights gained from sediment profile imaging technology regarding biological community structure and dynamics in sandy and coarse-grained bottoms are fairly limited.

2.1.5 Biological Mixing Depth

During the past two decades, there has been a considerable emphasis on studying the effects of bioturbation on sediment geotechnical properties as well as sediment diagenesis (Ekman et al., 1981; Nowell et al., 1981; Rhoads and Boyer, 1982; Grant et al., 1982; Boudreau, 1986; 1994; 1998). However, an increasing focus of research is centering on the rates of contaminant flux in sediments (Reible and Thibodeaux, 1999; François et al., 2002; Gilbert et al., 2003), and the two parameters that affect the time rate of contaminant flux the greatest are erosion and bioturbation (Reible and Thibodeaux, 1999). The depth to which sediments are bioturbated, or the biological mixing depth, can be an important parameter for studying either nutrient or contaminant flux in sediments. While the apparent RPD is one potential measure of biological mixing depth, it is quite common in

profile images to see evidence of biological activity (burrows, voids, or actual animals) well below the mean apparent RPD. Both the minimum and maximum linear distance from the sediment surface to both the shallowest and deepest feature of biological activity can be measured along with a notation of the type of biogenic structure measured. For this report, the maximum depth to which any biological activity was noted was measured and mapped.

.

3.0
RESULTS

While replicate images were taken at each station, the amount of disturbance caused by the diver-deployed system did not allow for reliable measurements of precision between the two replicate images, so only one replicate (the least disturbed) from each station sampled by divers was analyzed. The amount of debris in and around the piers coupled with the high density of shell fragments also created high variation in the penetration depth at the frame deployed stations, with cross-sectional sedimentary structures masked or destroyed by debris (natural or anthropogenic) being dragged down by the prism cutting blade. While a copy of all images collected was provided to the client, given the variation in image feature preservation (regardless of whether they were taken with the frame-deployed or diver-deployed system), and because this variation in cross-sectional structural appearance was not really indicative of natural variance in the measured parameters, the best image (least disturbed) from each station was analyzed. A complete set of all the summary data measured from each image is presented in Appendix A.

The results for some SPI parameters are sometimes indicated in the data appendix or on the maps as being "Indeterminate" (Ind). This is a result of the sediments being either: 1) too compact for the profile camera to penetrate adequately, preventing observation of surface or subsurface sediment features, 2) too soft to bear the weight of the camera, resulting in over-penetration to the point where the sediment/water interface was above the window (imaging area) on the camera prism (the sediment/water interface must be visible to measure most of the key SPI parameters like aRPD depth, penetration depth, and infaunal successional stage), or 3) the biogenic and sedimentary stratigraphic structure was compromised or destroyed by sampling artifacts caused by the divers inserting the prism into the sediment (either vibrating or wiggling the camera to achieve greater penetration, which allowed suspended sediment to collect in between the cross-sectional profile and the faceplate of the prism).

SPI has been shown to be a powerful reconnaissance tool that can efficiently map gradients in sediment type, biological communities, or disturbances from physical forces or organic enrichment. The results and conclusions in this report are about dynamic processes that have been deduced from imaged structures; as such, they should be considered hypotheses available for further testing/confirmation. By employing Occam's Razor, we feel reasonably assured that the most parsimonious explanation is usually the one borne out by subsequent data confirmation.

3.1 PRISM PENETRATION DEPTH

Sediments throughout the site ranged from silt-clays with minor fractions of very fine to fine sand in the rows that ran under the pier, to silty sands as one progressed beyond the pier into Transect #7 (Figure 5). The mean prism penetration depth in the study area ranged from 7.3 to 21.2 cm, with an overall site average of 14.8 cm; the spatial distribution of mean penetration depth at all stations sampled is shown in Figure 6.

3.2 APPARENT REDOX POTENTIAL DISCONTINUITY DEPTH

The distribution of mean apparent RPD depths is shown in Figure 7; mean aRPD depths could not be measured at 12 of the stations sampled by divers because of sampling artifacts that caused distortions to the sediment profile and eliminated the possibility of any accurate measurements. While two of the stations had such high sediment-oxygen demand that no detectable aRPD was present (Stations 2-4 and 3-3; see Figure 8), the remaining stations had values ranging from 0.5 to 4.2 cm, with an overall site average of 1.8 cm.

3.3 INFAUNAL SUCCESSIONAL STAGE

The mapped distribution of infaunal successional stages is shown in Figure 9; while many of the stations had a surface armoring of shell-hash along with shell fragments mixed throughout the sediment column, presence of Stage 3 taxa (infaunal deposit feeders) was evident at 26 of the 42 stations. All of the stations outboard of the pier, e.g. 1-4, 2-4, 3-4, 4-4, etc., had dense assemblages of tubes from large sabellid polychaetes (Figure 10) that had evidently colonized the area from being removed from the bottom of ship hulls and established themselves in the sediments in the berthing areas; no sabellids were found in any of the images taken underneath the pier.

3.4 MAXIMUM BIOLOGICAL MIXING DEPTH

The spatial distribution of the maximum depth to which any biological activity was seen in the study area is shown in Figure 11. Evidence of infaunal burrowing was seen even in some of the images where the cross-sectional features of the profile were disturbed by diver sampling; maximum depth of biogenic activity ranged from 4.1 to 19.1 cm, with an overall site average of 12.7 cm for the maximum biological mixing depth.

4.0
DISCUSSION

The results from the SPI technology survey from the area around Pier 7 at the PSNS & IMF Bremerton site will serve as a good record of baseline conditions prior to the placement of the activated cap amendment. The most unusual finding from this baseline survey was the narrow band of the dense assemblage of sabellids alongside of the floating pontoon just to the west of the pier (concentrated in the location of station 4 in each of the transect rows); while these polychaetes were most likely brought to this area of bottom by originally being attached to ship's hulls, their distribution is rather localized and appears to be confined to the original footprint of their deposit from the hull and re-establishment on the sediment surface immediately under where the ships were docked.

While it was difficult to get accurate measurements of subsurface features from the images collected by divers (Figure 12) from locations under the pier , the widespread presence of infaunal deposit feeders throughout the site (Figure 9) should insure that adequate biogenic mixing of the amendment will occur after placement. It may prove difficult to accurately assess mixing of the amended cap material at the stations from under the pier that will be sampled by divers, but hopefully they will be able to improve their "prism insertion" techniques in future survey with more practice. We do not anticipate any issues with measuring the presence and depth to which the cap is mixed at those stations sampled from the boat with the support frame.

5.0
REFERENCES CITED

Boudreau, B.P. 1986. Mathematics of tracer mixing in sediment. I-Spatially-dependent, diffusive mixing. II: Non-local mixing and biological conveyor-belt phenomena. Am. Jour. Sci. 286: 161-238.

Boudreau, B.P. 1994. Is burial velocity a master parameter for bioturbation? Geochimica et Cosmochemica Acta 58: 1243-1249.

Boudreau, B. P. 1998. Mean mixed depth of sediments: The wherefore and the why. Limnol. Oceanogr. 43: 524-526.

Diaz, R. J. and L. C. Schaffner. 1988. Comparison of sediment landscapes in the Chesapeake Bay as seen by surface and profile imaging, p. 222-240 In M. P. Lynch and E. C. Krome (eds.), Understanding the Estuary: Advances in Chesapeake Bay Research, Chesapeake Bay Research Consortium Publication 129, Chesapeake Bay Program 24/88.

Ekman, J.E., Nowell, A.R.M., and P.A. Jumars. 1981. Sediment destabilization by animal tubes. J. Mar. Res. 39: 361-374.

Fenchel, T. 1969. The ecology of marine macrobenthos IV. Structure and function of the benthic ecosystem, its chemical and physical factors and the microfauna communities with special reference to the ciliated protozoa. Ophelia 6: 1-182.

François, F., Gerino, M., Stora, G., Durbec, J.P., and J.C. Poggiale. 2002. Functional approach to sediment reworking by gallery-forming macrobenthic organisms: modeling and application with the polychaete *Nereis diversicolor*. Marine Ecology Progress Series 229: 127–136.

Fredette, T.J., W.F. Bohlen, D.C. Rhoads, and R.W. Morton. 1988. Erosion and resuspension effects of Hurricane Gloria at Long Island Sound dredged material disposal sites. In: Proceedings of the Water Quality ‘88 seminar, February Meeting, Charleston, South Carolina. U.S. Army Corps of Engineers, Hydraulic Engineering Center, Davis, CA.

Germano, J.D. 1983. Infaunal succession in Long Island Sound: Animal-sediment interactions and the effects of predation. Ph.D. dissertation. Yale University, New Haven, CT. 206 pp.

Germano, J.D. and D.C. Rhoads. 1984. REMOTS sediment profiling at the Field Verification Program (FVP) Disposal Site. In: Dredging '84 Proceedings, ASCE, Nov. 14-16, Clearwater, FL. pp. 536-544.

Germano, J.D., D.C. Rhoads, R.M. Valente, D.A. Carey, and M. Solan. 2011. The use of Sediment Profile Imaging (SPI) for environmental impact assessments and monitoring studies – lessons learned from the past four decades. Oceanography and Marine Biology: An Annual Review 49: 247-310.

Gilbert, F. S. Hulth, N. Strömberg, K. Ringdahl, and J.-C. Poggiale. 2003. 2-D optical quantification of particle reworking activities in marine surface sediments. Jour. Exp. Mar. Biol. Ecol. 285-286: 251-264.

Grant, W.D., Jr., Boyer, L.F., and Sanford, L.P. 1982. The effects of bioturbation on the initiation of motion of intertidal sands: Jour. Mar. Res., Vol. 40, pp. 659-677.

Horn, H.S. 1974. The ecology of secondary succession. Ann. Rev. Ecol. Syst. 5: 25-37.

Huettel, M., Ziebis, W., Forster., S., and G.W. Luther III. 1998. Advective transport affecting metal and nutrient distributions and interfacial fluxes in permeable sediments. Geochimica et Cosmochemica Acta 62: 613-631.

Lyle, M. 1983. The brown-green colour transition in marine sediments: A marker of the Fe (III) – Fe(II) redox boundary. Limnol. Oceanogr. 28: 1026-1033.

Nowell, A.R.M., P.A. Jumars, and J.E. Ekman. 1981. Effects of biological activity on the entrainment of marine sediments. Mar. Geol. 42: 133-153.

Painter, T.H., M. E. Schaepman, W. Schweizer, and J. Brazile. 2007. Spectroscopic discrimination of shit from shinola. Annals of Improbable Research 13: 22-23.

Pearson, T.H. and R. Rosenberg. 1978. Macrobenthic succession in relation to organic enrichment and pollution of the marine environment. Oceanogr. Mar. Biol. Ann. Rev. 16:229-311.

Reible, D and Thibodeaux, L. 1999. Using Natural Processes to Define Exposure From Sediments., in Sediment Management Work Group; Contaminated Sediment Management Technical Papers, Sediment Management Work Group, http://www.smwg.org/index.htm.

Revelas, E.C., J.D. Germano, and D.C. Rhoads. 1987. REMOTS reconnaissance of benthic environments. pp. 2069-2083. In: Coastal Zone ‘87 Proceedings, ASCE, WW Division, May 26-29, Seattle, WA.

Rhoads, D.C. 1974. Organism-sediment relations on the muddy seafloor. Oceanogr. Mar. Biol. Ann. Rev. 12: 263-300.

Rhoads, D.C. and L.F. Boyer. 1982. The effects of marine benthos on physical properties of sediments. pp. 3-52. In: Animal-Sediment Relations. McCall, P.L. and M.J.S. Tevesz (eds). Plenum Press, New York, NY.

Rhoads, D.C. and J.D. Germano. 1982. Characterization of benthic processes using sediment profile imaging: An efficient method of remote ecological monitoring of the seafloor (REMOTS™ System). Mar. Ecol. Prog. Ser. 8:115-128.

Rhoads, D.C. and J.D. Germano. 1986. Interpreting long-term changes in benthic community structure: A new protocol. Hydrobiologia. 142:291-308.

Rhoads, D.C. and J.D. Germano. 1990. The use of REMOTS® imaging technology for disposal site selection and monitoring. pp. 50-64. In: Geotechnical Engineering of Ocean Waste Disposal, K. Demars and R. Chaney (eds). ASTM Symposium Volume, January, 1989. Orlando, FL.

Rosenberg, R., H.C. Nilsson, and R.J. Diaz. 2001. Response of benthic fauna and changing sediment redox profiles over a hypoxic gradient. Estuarine, Coastal and Shelf Science 53: 343-350.

Valente, R.M., D.C. Rhoads, J.D. Germano, and V.J. Cabelli. 1992. Mapping of benthic enrichment patterns in Narragansett Bay, RI. Estuaries 15:1-17.

Ziebis, W., Huettel, M., and S. Forster. 1996. Impact of biogenic sediment topography on oxygen fluxes in permeable seabeds. Mar. Ecol. Prog. Ser. 140: 227-237.

FIGURES

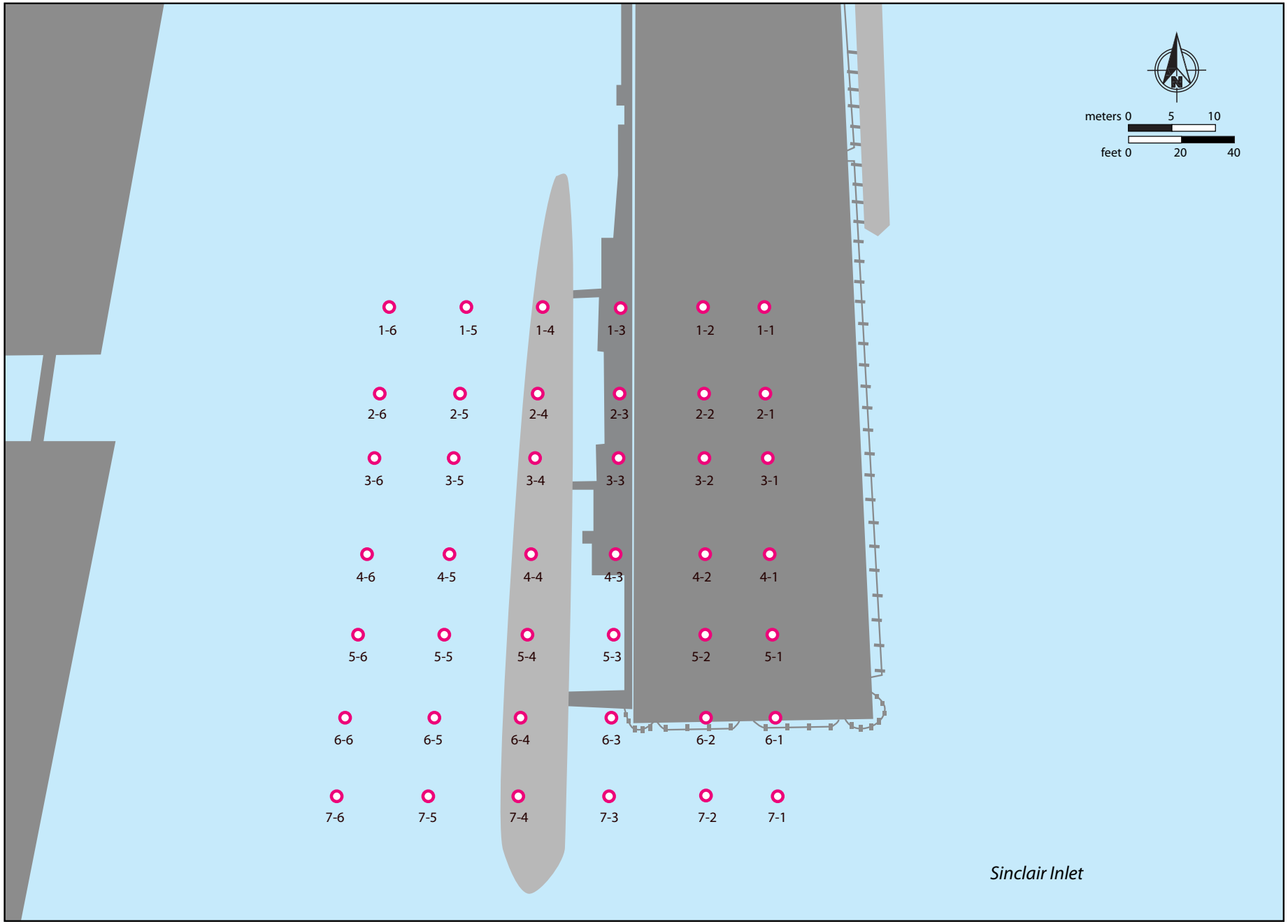

Figure 1: Location of SPI stations under and around Pier 7 at the Puget Sound Naval Shipyard & Intermediate Maintenance Facility, Bremerton, WA.

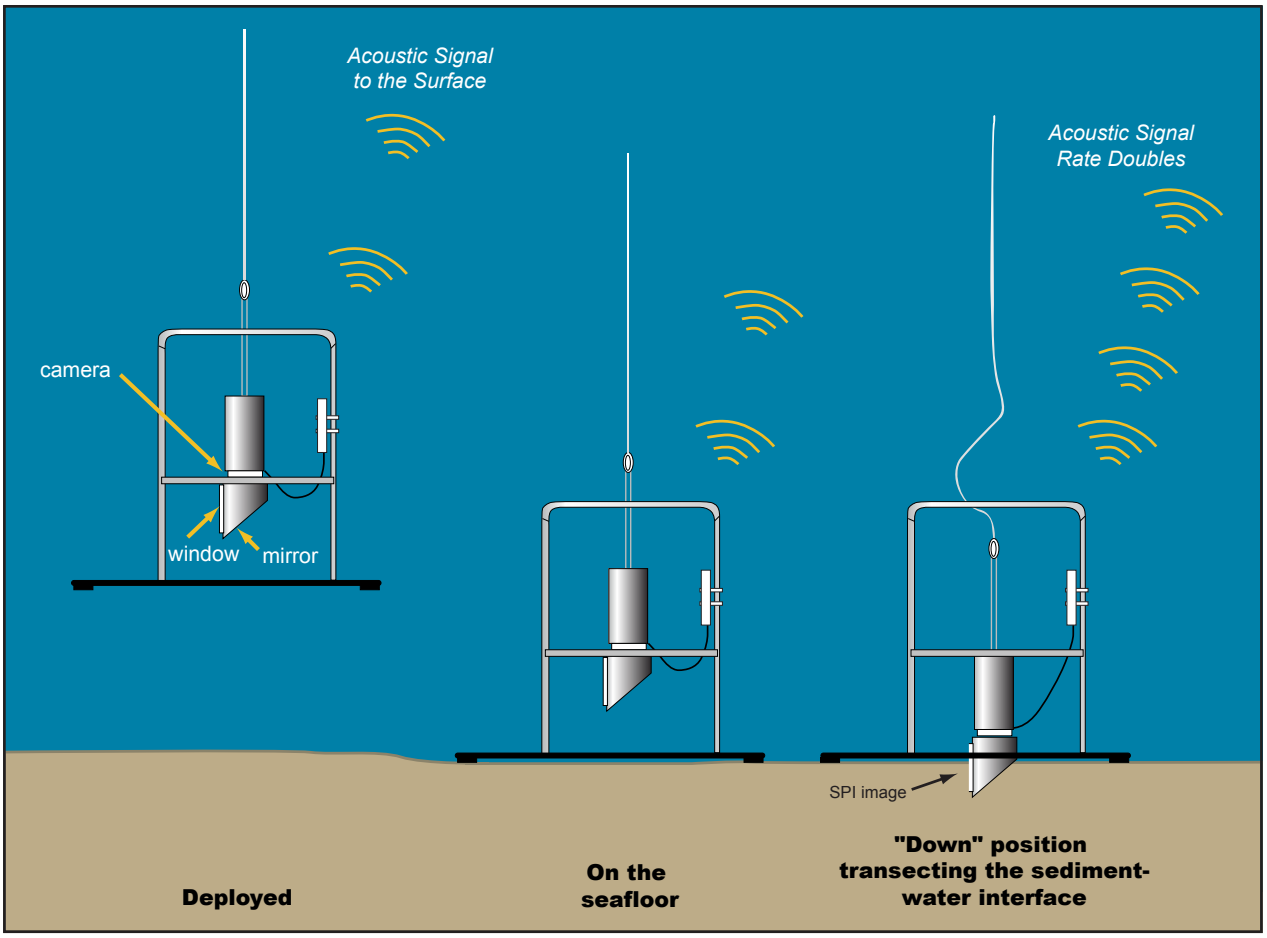

Figure 2: Deployment and operation of the SPI camera system. The central cradle of the camera is held in the “up” position by tension on the winch wire as it is being lowered to the seafloor (left); once the frame base hits the bottom (center), the prism is then free to penetrate the bottom (right) and take the photograph.

Figure 3: The hand-held SPI system used by divers for all stations that were located underneath Pier 7 at PSNS & IMF Bremerton site.

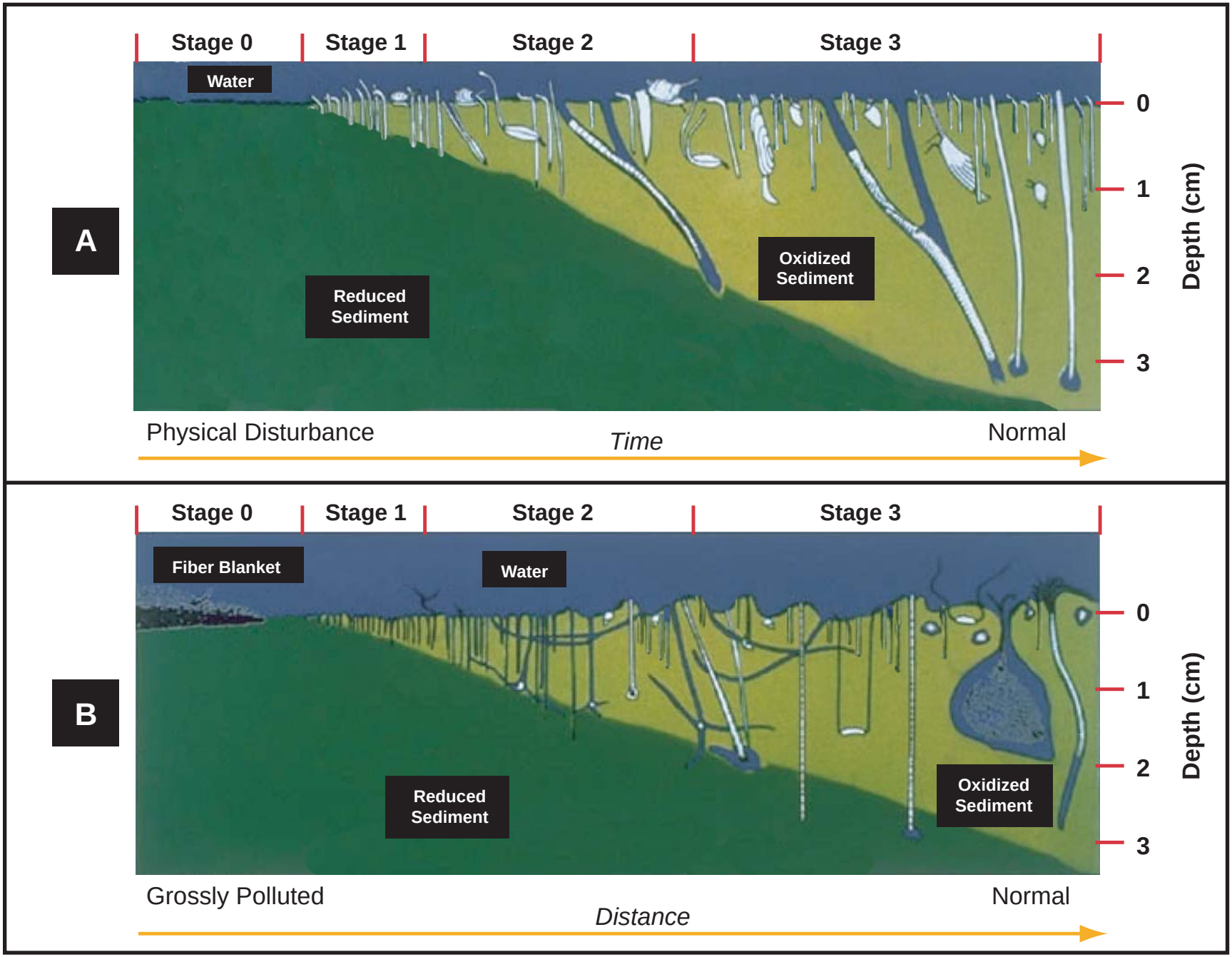

Figure 4: The stages of infaunal succession as a response of soft-bottom benthic communities to physical disturbance (top panel) or organic enrichment (bottom panel). From Rhoads and Germano, 1982.

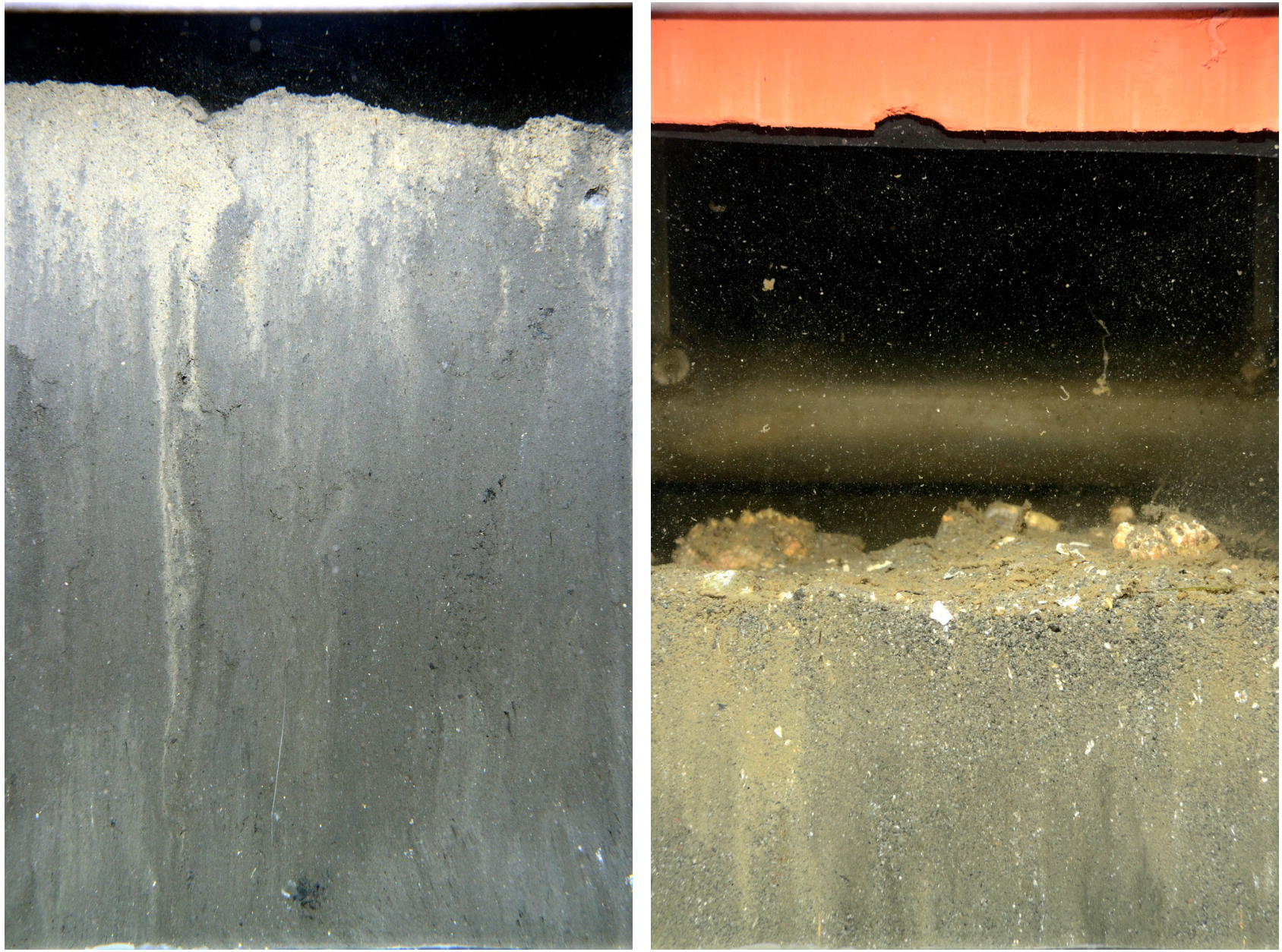

1-5 7-3

Figure 5: Camera prism penetration was notably deeper in the finer-grained stations such as at Station 1-5 (left) as compared with stations at the southern end of the grid that had a higher sand fraction as seen in this profile image from Station 7-3 (right). Scale: width of each image = 14.5 cm. Note: Orange band on top of right image is from the rubber faceplate wiper on the SPI system.

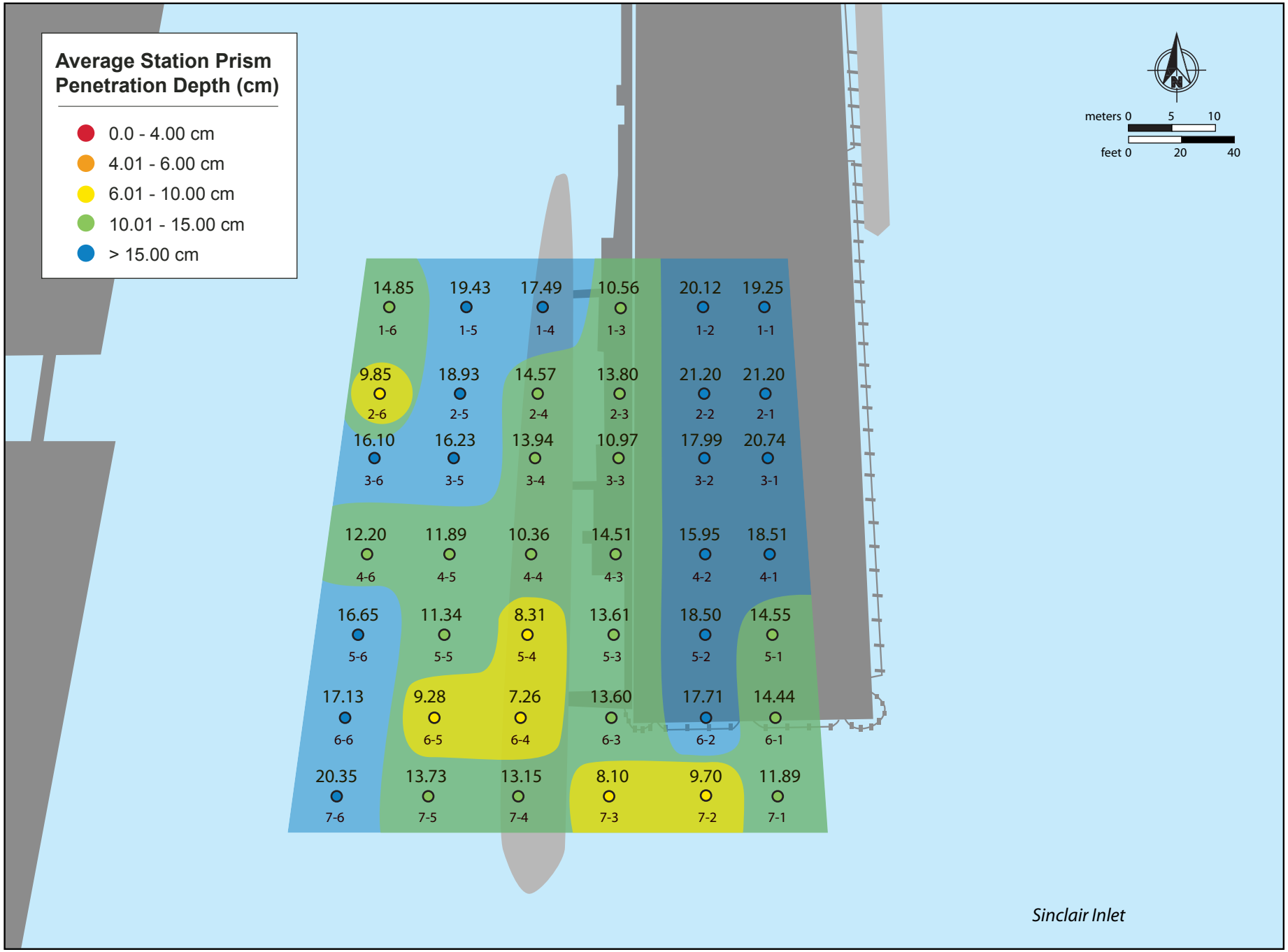

Figure 6: Spatial distribution of mean prism penetration depth (cm) at Pier 7 at the PSNS & IMF Bremerton site in August, 2012.

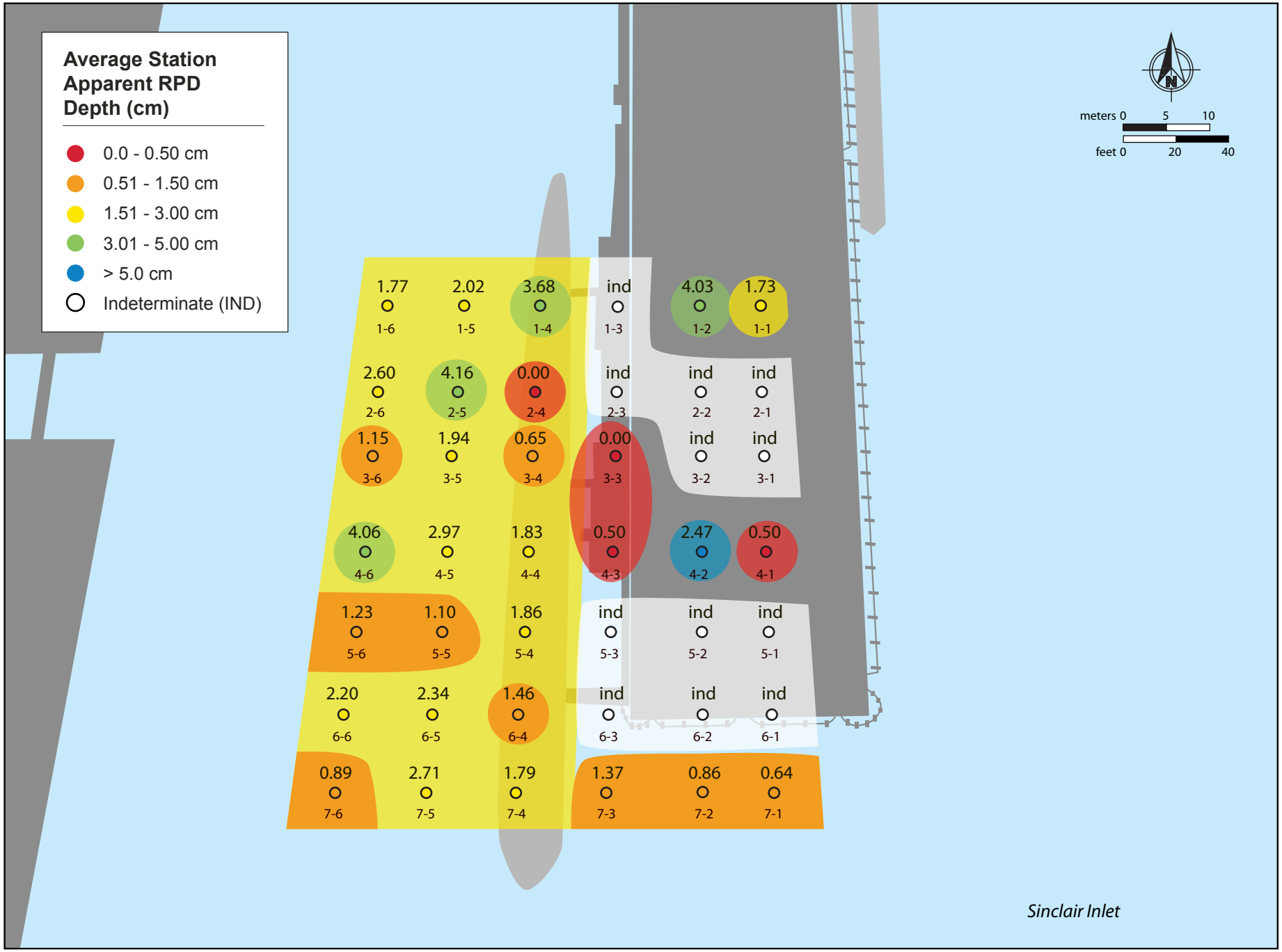

Figure 7: Spatial distribution of apparent RPD depth (cm) at Pier 7 at the PSNS & IMF Bremerton site in August, 2012.

Figure 8: This profile image from Station 2-4 shows sabellid polychaete tubes projecting above a high-organic content sediment with no detectable surface oxidized layer. Scale: width of profile image = 14.5 cm.

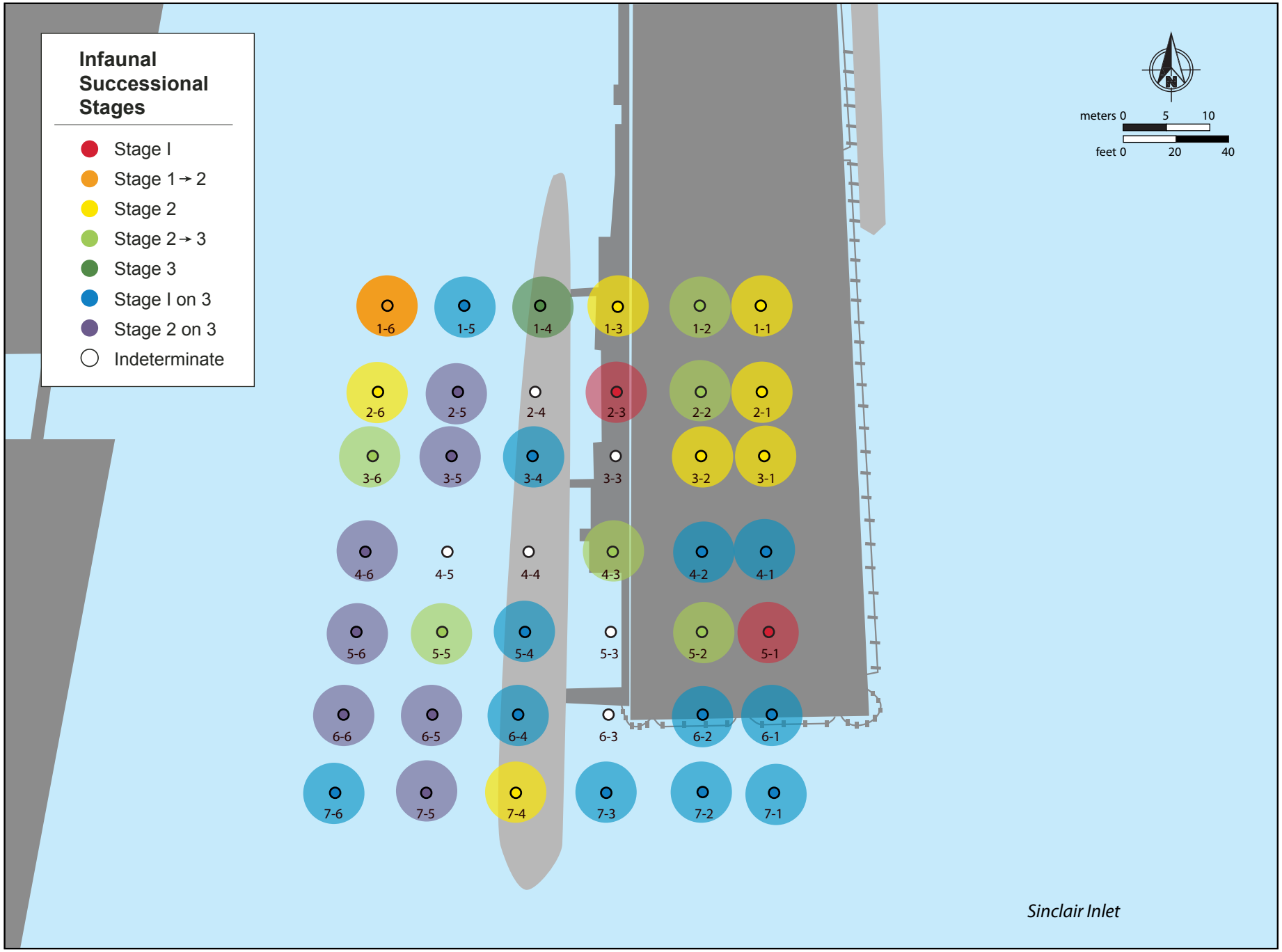

Figure 9: Spatial distribution of infaunal successional stage at the locations sampled around Pier 7 at the PSNS & IMF Bremerton site in August, 2012.

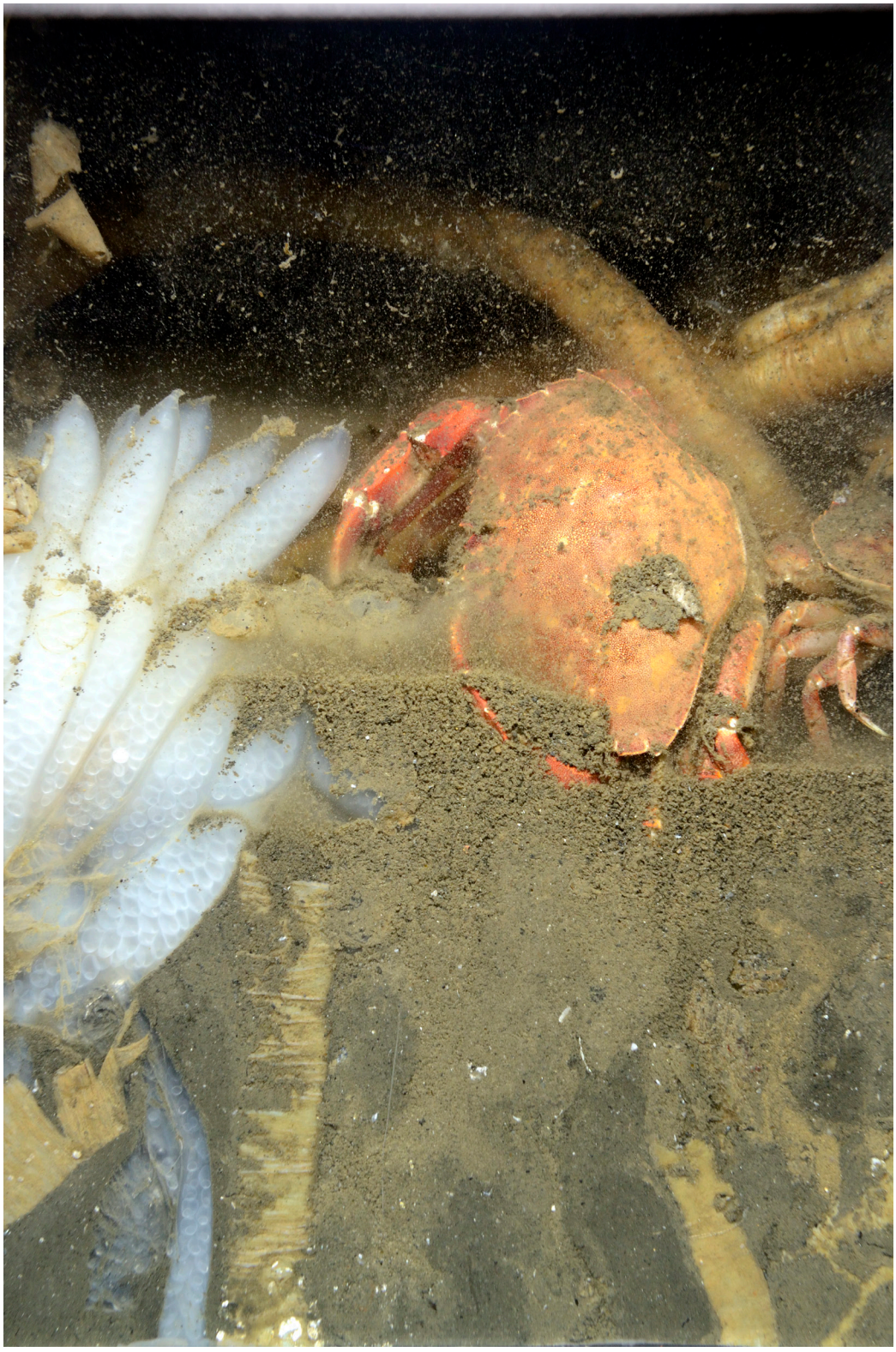

Figure 10: This profile image from Station 4-4 is an excellent example of the size and density of the tubes from sabellid polychaetes that were quite common at locations to the west of the pier. Squid eggs (white casings) and graceful crabs are also clearly visible. Scale: width of profile image = 14.5 cm.

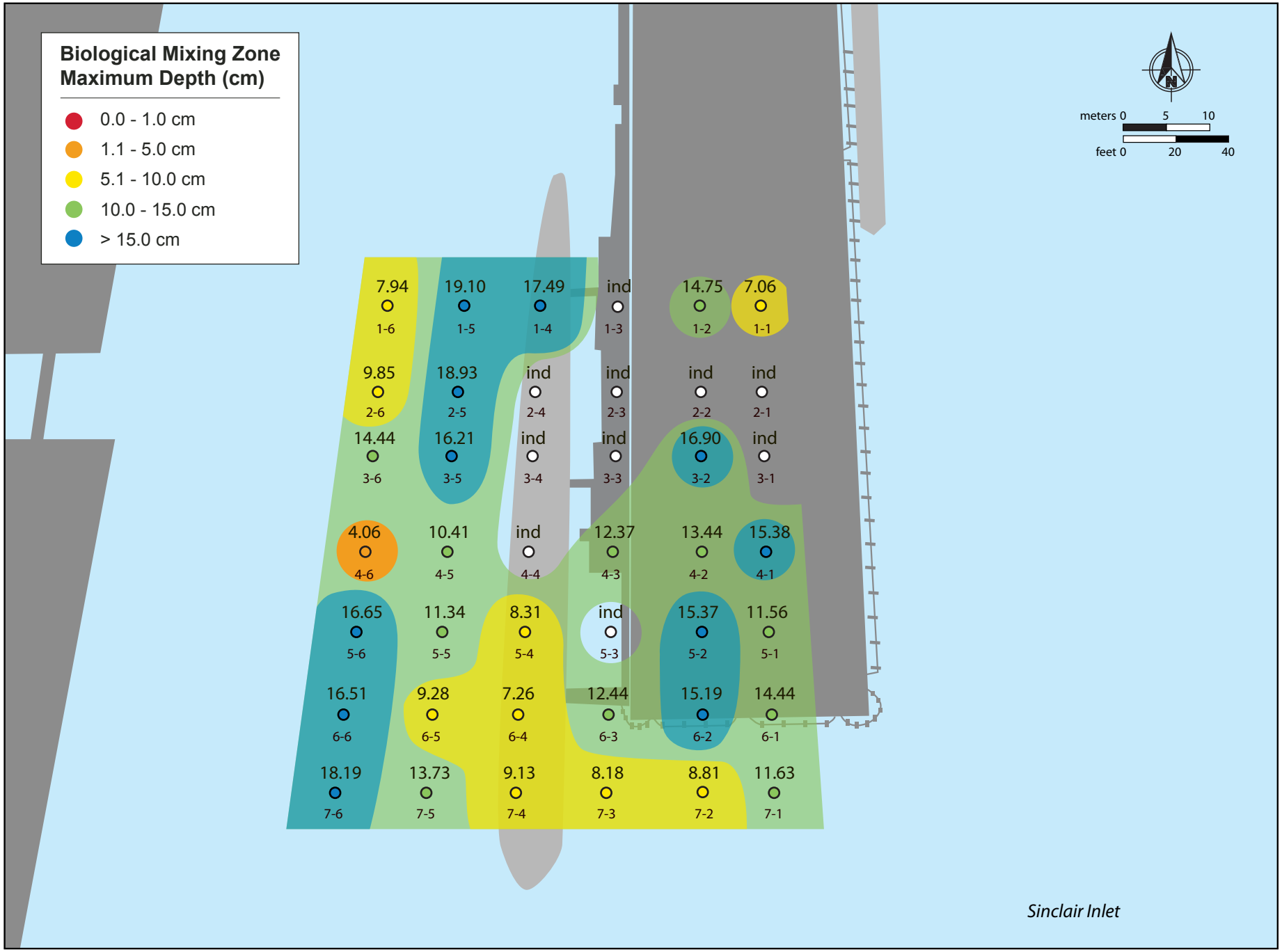

Figure 11: Spatial distribution of maximum biological mixing depth (cm) at Pier 7 at the PSNS & IMF Bremerton site in August, 2012.

Figure 12: This profile image from Station 1-3 is typical of many of the images collected by divers and shows the lack of preservation of any subsurface features due to the prism being wiggled to insert it in the sediment. Scale: width of image = 14.5 cm.

APPENDIX A

Sediment Profile Image Analysis Results

STATION	REP	DATE	TIME	Calibration Constant	Penetration Area (sq.cm)	Average Penetration (cm)	RPD Area (sq.cm)	Mean RPD (cm)	Bio Mixing Zone Max Depth (cm)	Successional Stage	COMMENT
PSNS-1-1	A	8/16/2012	9:27:58	14.455	278.29	19.25	25.04	1.73	7.06	Stage 2	Sandy silt, with lots of shell fragments incorporated in upper cms; broken shells (various, some mussel) on surface; evidence of shallow burrows
PSNS-1-2	A2	8/16/2012	9:33:56	14.455	290.77	20.12	58.27	4.03	14.75	Stage 2 -> 3	Sandy silt with some shell fragments incorporated in upper oxy cms; top of SWI not visible on left; smear and dragdown to right; few mussel shell halves against faceplate; area of settled fine pellets at surface on right; v. small burrows in oxy sed to right to depth
PSNS-1-3	A	8/16/2012	9:45:41	14.455	152.69	10.56	Ind	ind	ind	Stage 2	Sandy silt, aRPD indeterminate because of surface disturbance by divers; large shells on surface, also mussel shells; shell fragments incorporated throughout image. Shallow burrowing with portions of infauna visible; aRPD most likely diffusional given high SOD of sediment.
PSNS-1-4	A	8/17/2012	8:01:24	14.425	252.26	17.49	53.05	3.68	17.49	Stage 3	Silt-clay with minor fraction of very fine sand; fecal pellet layer at surface, sabellid worms visible, evidence of reworking to full depth of image
PSNS-1-5	B	8/17/2012	9:28:13	14.425	280.27	19.43	29.21	2.02	19.10	Stage 1 on 3	Silt-clay; dense small tubes @ SWI, small burrows in aRPD and evidence of deeper burrowing throughout profile
PSNS-1-6	C	8/17/2012	12:27:12	14.425	214.24	14.85	25.53	1.77	7.94	Stage 1 -> 2	Silt-clay; distinct aRPD; fecal pellet surface layer & portions of small polychaetes visible in profile.
PSNS-2-1	B	8/16/2012	10:11:01	14.455	306.44	21.20	Ind	ind	ind	Stage 2	Overpenetration of silt-clay with high fraction of shell hash & fragments incorporated through most of sediment depth; few chunks of oxidized sed at ~1cm near surface; profile disturbed by divers and most of the visible subsurface structure is artifact of sampling.
PSNS-2-2	A2	8/16/2012	10:13:13	14.455	277.69	21.20	Ind	ind	ind	Stage 2 -> 3	Overpenetration of silt-clay with high fraction of shell hash & fragments incorporated through most of sediment depth; profile disturbed by divers and most of the visible subsurface structure is artifact of sampling. Evidence of burrowing at depth
PSNS-2-3	A2	8/16/2012	10:22:00	14.455	199.55	13.80	ind	ind	ind	Stage 1	Silt-clay with shell fragments incorporated through most of sediment depth; lots of larger shells on surface, mussels and others, some with barnacles on them, possible rocks in background; Beggiatoa filaments visible in sediment, high SOD.
PSNS-2-4	A	8/17/2012	8:11:57	14.425	210.25	14.57	0.00	0.00	ind	indeterminate	High SOD silt-clay with minor fraction of very fine sand, 2 sabellids from depth to surface, an additional tube on surface that is dead (gray in color); traces of Beggiatoa on tube surface, so low dissolved O2 in boundary layer.
PSNS-2-5	A	8/17/2012	9:42:49	14.425	273.06	18.93	59.98	4.16	18.93	Stage 2 on 3	Silt-clay with minor vfs fraction, distinct aRPD; bits of small polychaetes against faceplate at depth; sabellid tube above surface and through to depth on right
PSNS-2-6	A	8/17/2012	12:14:26	14.425	142.16	9.85	37.55	2.60	9.85	Stage 2	Silt-clay with minor vfs fraction; distinct aRPD; fecal pellets at surface and in upper cm; small burrows in aRPD
PSNS-3-1	B	8/16/2012	10:38:54	14.455	299.82	20.74	ind	ind	ind	Stage 2	Sandy silt with small shell fragments incorporated through depth; aRPD is not distinct and profile disturbed by sampling artifact.
PSNS-3-2	B	8/16/2012	10:42:17	14.455	260.11	17.99	ind	ind	16.90	Stage 2	Silty sediment; lots of shell frag, blanketing surface, incorporated heavily in upper 3-4 cm; aRPD is not distinct, most likely diffusional layer of oxidized surface particles dragged down over underlying profile by sampling artifact.
PSNS-3-3	B	8/16/2012	10:48:06	14.455	158.56	10.97	0.00	0.00	ind	indeterminate	Sandy silt with dense shell fragments throughout, particularly in the lower right; topped with fine layer of sed at surface; high SOD, Beggiatoa colonies present, profile disturbed by diver sampling artifact so biogenic mixing zone indeterminate.
PSNS-3-4	B	8/17/2012	8:26:15	14.425	201.12	13.94	9.31	0.65	ind	Stage 1 on 3	Sandy silt; large apparent burrow extending from surface to depth is artifact of surface bivalve shell being dragged down by camera prism and disturbing profile; somewhat patchy aRPD with small thin burrows.
PSNS-3-5	C	8/17/2012	10:07:20	14.425	234.10	16.23	27.95	1.94	16.21	Stage 2 on 3	Sandy silt with small burrows in upper cms of aRPD; void at depth
PSNS-3-6	A	8/17/2012	11:50:46	14.425	232.26	16.10	16.56	1.15	14.44	Stage 2 -> 3	Sandy silt with small burrows in oxidized layer and evidence of burrowing at depth.
PSNS-4-1	A	8/16/2012	11:42:48	14.455	267.59	18.51	7.28	0.50	15.38	Stage 1 on 3	Sandy silt with small shell fragments incorporated through entire profile; small gastropod on surface; aRPD is not distinct; few thin polychaetes visible in upper 7 cm, evidence of burrowing at depth as well as Beggiatoa filaments throughout profile.
PSNS-4-2	B	8/16/2012	11:50:48	14.455	230.56	15.95	35.66	2.47	13.44	Stage 1 on 3	Silty sediment, shell fragments incorporated in upper few cms with smaller shell bits to depth; larger shell fragments at surface, v. fine sed & fecal pellets at surface; polychaete visible on right at depth ~7cm. Beggiatoa filaments visible.
PSNS-4-3	A	8/16/2012	11:56:38	14.455	209.79	14.51	7.22	0.50	12.37	Stage 2 -> 3	Silty sediment, with some coarser grains and shell fragments incorporated; surface covered with cobble and shell; layers of shell frag/cobbles at 0.5cm; v fine sed in this layer on surface; two polychaetes visible below aRPD at ~2.5cm; relict aRPD, Beggiatoa filaments present
PSNS-4-4	B	8/17/2012	8:44:17	14.425	149.43	10.36	26.34	1.83	ind	indeterminate	Silt with oxidized pellet layer on surface; two crabs on surface; at least 3 sabellid worm tubes in sed, couple extend on surface; clusters of squid eggs that were dragged down to entire depth of image by prism (artifact).
PSNS-4-5	C	8/17/2012	10:18:07	14.425	171.56	11.89	42.89	2.97	10.41	indeterminate	Silt, with some coarse sediment; surface is uneven from crab being pushed below sediment by camera; most of profile cross sectional structure is sampling artifact.
PSNS-4-6	B	8/17/2012	11:36:28	14.425	176.01	12.20	58.56	4.06	4.06	Stage 2 on 3	Sandy silt, wide burrow connected to surface with some debris covered in sed at surface and filled with reworked sed, small burrows in upper cm.
PSNS-5-1	B	8/16/2012	12:10:27	14.455	210.39	14.55	Ind	ind	11.56	Stage 1	Sandy silt with high proportion of shell fragments incorporated throughout most of profile; surface layer of fecal pellets, aRPD appears diffusional with Beggiatoa colonies present at surface; however, evidence of burrowing at depth. Profile disturbed by divers.
PSNS-5-2	B	8/16/2012	12:14:03	14.455	267.48	18.50	Ind	ind	15.37	Stage 2 -> 3	Sandy silt with lots of shell fragments incorporated throughout sediment depth; few larger shell fragments at surface; no clear aRPD, profile disturbed by diver insertion of prism. Evidence of subsurface burrowing clearly visible at depth.
PSNS-5-3	A	8/16/2012	12:18:10	14.455	196.68	13.61	Ind	ind	ind	indeterminate	Sandy silt with high proportion of shell fragments; thick cloud of dark suspended sed obscuring much of SWI; profile disturbed by diver insertion, no cross-sectional original features preserved.
PSNS-5-4	B	8/17/2012	8:57:21	14.425	119.85	8.31	26.83	1.86	8.31	Stage 1 on 3	Silt-clay with minor sand fraction; clump of sabellid tubes on right, one extending across width of image, at least one is clearly empty; some coarse sand below reworked sed just below surface; small burrows in aRPD and evidence of burrowing at depth.
PSNS-5-5	A	8/17/2012	10:22:16	14.425	163.61	11.34	15.86	1.10	11.34	Stage 2 -> 3	Silty fine sand; distinct aRPD; polychaete visible near base of aRPD to left of center, evidence of burrowing at depth.
PSNS-5-6	A	8/17/2012	11:30:01	14.425	240.25	16.65	17.81	1.23	16.65	Stage 2 on 3	Silty fine sand with coarser grains near surface; several polychaetes against faceplate below aRPD and at depth.
PSNS-6-1	A	8/16/2012	12:45:24	14.455	208.80	14.44	ind	ind	14.44	Stage 1 on 3	Sandy silt with high proportion of shell fragments incorporated throughout sediment depth; surface covered with shell hash; polychaete visible against faceplate, evidence of burrowing to depth. Profile structure/aRPD distorted from diver insertion.
PSNS-6-2	B	8/16/2012	12:53:25	14.455	255.98	17.71	ind	ind	15.19	Stage 1 on 3	Sandy silt with great deal of shell fragments incorporated throughout the sediment depth, dense and larger fragments in upper few cms; surface covered with thick layer of shell hash. Layer of oxidized fecal pellets at surface, no distinct aRPD (structure obliterated by divers); polychaete at depth
PSNS-6-3	B	8/16/2012	12:57:38	14.455	196.55	13.60	ind	ind	12.44	indeterminate	Sandy silt with great deal of shell fragments incorporated throughout the sediment depth, dense and larger fragments in upper few cms; surface covered with thick layer of shell hash. Layer of oxidized fecal pellets at surface, no distinct aRPD (structure obliterated by divers).

STATION	REP	DATE	TIME	Calibration Constant	Penetration Area (sq.cm)	Average Penetration (cm)	RPD Area (sq.cm)	Mean RPD (cm)	Bio Mixing Zone Max Depth (cm)	Successional Stage	COMMENT
PSNS-6-4	B	8/17/2012	9:05:46	14.425	104.69	7.26	21.01	1.46	7.26	Stage 1 on 3	Silt-clay with minor fraction of fine sand; few sabellid tubes in sed and on surface, some thin burrows in upper cm
PSNS-6-5	A	8/17/2012	10:50:30	14.425	133.84	9.28	33.83	2.34	9.28	Stage 2 on 3	Silty fine sand with coarser grains near surface; some organic debris at surface; small burrows within aRPD; polychaete at depth.
PSNS-6-6	A	8/17/2012	11:17:19	14.425	247.06	17.13	31.75	2.20	16.51	Stage 2 on 3	Silty very fine sand, small and large polychaetes at depth; evidence of burrowing throughout profile
PSNS-7-1	A	8/16/2012	14:38:41	14.455	171.92	11.89	9.27	0.64	11.63	Stage 1 on 3	Silty very fine sand with coarser grains in upper cm; depression, few large shell fragments on surface and other organic debris, evidence of burrowing throughout profile.
PSNS-7-2	C	8/16/2012	14:26:58	14.455	140.16	9.70	12.49	0.86	8.81	Stage 1 on 3	Sandy silt; surface covered with shells (one open mussel, other barnacle covered shells); discontinuous aRPD, only on right side; fecal pellets at surface, evidence of burrowing at depth.
PSNS-7-3	B	8/16/2012	14:08:25	14.455	117.10	8.10	19.87	1.37	8.18	Stage 1 on 3	Silty fine sand, coarser at surface; surface covered with small organic debris and larger shells or rocks; two small polychaetes against faceplate at depth, evidence of burrowing throughout profile.
PSNS-7-4	C	8/17/2012	12:59:09	14.425	189.73	13.15	25.82	1.79	9.13	Stage 2	Silt; organic debris at surface; sabellid worm tube gragement on surface; 3 sabellid tubes dragged down by prism.
PSNS-7-5	C	8/17/2012	13:09:03	14.425	198.01	13.73	39.13	2.71	13.73	Stage 2 on 3	Silty fine sand; distinct aRPD; two polychates against faceplate at depth; small open end of large burrow below aRPD; evidence of burrowing to depth
PSNS-7-6	C	8/17/2012	13:26:38	14.425	293.57	20.35	12.86	0.89	18.19	Stage 1 on 3	Sandy silt; small polychaete against faceplate at depth, evidence of burrowing throughout profile